SYNTHESIS, STRUCTURAL AND OPTICAL CHARACTERIZATION OF NOVEL DONOR-π-ACCEPTOR BRIDGED ANTHRACENYL-CHALCONES FOR NONLINEAR OPTICAL MATERIALS

SITI NOOR FARHANA BINTI AB RAHMAN

UNIVERSITI SAINS MALAYSIA

2024

SYNTHESIS, STRUCTURAL AND OPTICAL CHARACTERIZATION OF NOVEL DONOR-π-ACCEPTOR BRIDGED ANTHRACENYL-CHALCONES FOR NONLINEAR OPTICAL MATERIALS

by

SITI NOOR FARHANA BINTI AB RAHMAN

Thesis submitted in fulfilment of the requirements
for the degree of
Master of Science

September 2024

ACKNOWLEDGEMENT

I attribute the success of this work to Allah, the Most Merciful and Most Compassionate, for His blessings and guidance throughout this academic journey.

In the pursuit of knowledge and the completion of this master's dissertation, I am profoundly grateful to my supervisor, Prof. Dr. Abdul Razak Ibrahim, whose patience, continuous supervision, guidance, advice, wisdom, and support in completing this thesis have been a source of inspiration.

I express my humble gratitude to my co-supervisors, Dr. Suhana Arshad, and Dr. Mundzir Abdullah for their willingness to spare me their time and guide me in completing my study. They are the backbone of this research work, with their wonderful suggestions and constructive criticism. I extend my special gratitude to Dr. Dian Alwani Zainuri for her invaluable encouragement and insightful comments, which played a pivotal role in providing the motivation and guidance needed to bring this thesis to completion.

I want to take a moment to express my deepest gratitude and heartfelt thanks to my family members, especially my Abah and Umie, Ustaz Ab. Rahman and Mrs. Zainun, also my grandparents, Atok and Nenek, for their endless prayers, support, encouragement, patience, and love. To my lovely siblings and in-laws, thank you for being there; the unwavering support, kindness, love, and generosity have made a significant impact on my life, and I am truly grateful for your presence.

I express my sincere gratitude to my fellow lab colleagues and friends, Ms.Aliya, Ms. Farah, Ms. Rineswary, Ms. Aisyah, Mr. Aizat, Mr. Amin, Mr. Saleh and Ms. Wong Qin Ai who always helped me and shared their options and ideas in my research. I would also like to express my appreciation to all the X-ray Crystallography

laboratory staff, Mr. Mustaqim Rosli, Mr. Mustaqim Abu Bakar and Mr. Aswafi for their assistance and guidance in completing my master project. I would like to express my gratitude to Mr. Fikri and Mrs. Ainizatul for their great advice and help in the early stages of my master's program.

To the University Sains Malaysia and the X-ray Crystallography Laboratory, I express my gratitude for providing the academic environment and resources essential for this research. I would like to thank the Malaysian government and the University of Sains Malaysia for funding my studies through the Research University Grant (No: 203.PFIZIK.6711767).

I want to convey my heartfelt appreciation to everyone who has played a role, big or small, in contributing to the success of this study. Your support and assistance have been invaluable, and I am truly thankful. Thank you very much! Your contributions have made a significant difference, and you are truly the best!

TABLE OF CONTENTS

LIST OF TABLES

Page

LIST OF FIGURES

Page

LIST OF SYMBOLS

β	Nonlinear Absorption Coefficients
α	Linear Absorption Coefficient
$Re\chi^{(3)}$	The Real Parts of The Third-Order NLO Susceptibility
$Im\ \chi^{(3)}$	Imaginary Parts of The Third-Order NLO Susceptibility
λ	Wavelength
S	The Aperture Linear Transmittance
L	Thickness of the Sample.
k	Wave Vector.
f	Focal Point
c	Light Velocity in Vacuum.
$\|\Delta\varphi_o\|$	On-Axis Phase Shift at The Focus
ω_o	Beam Radius at The Aperture in Linear Regime.
ω_o	Beam Waist Radius at The Focal Point
$\chi^{(3)}$	Third-Order Nonlinear Susceptibility
ε_o	Vacuum Permittivity
z_R	Diffraction Length of The Beam
r_o	Aperture Radius
L_{eff}	Effective Thickness of The Sample
I_o	Intensity Of the Laser Beam at Focus Z=0

LIST OF ABBREVIATIONS

A	Acceptor
CCDC	The Cambridge Crystallographic Data Centre
CIF	Crystallographic Information File
CW	Continuous Wave
D	Donor
DFT	Density Functional Theory
DMSO	Dimethyl Sulfoxide
DPSS	Diode Pumped Solid State
FMOs	The Frontier Molecular Orbitals
HOMO	Highest Occupied Molecular Orbitals
ICT	Intermolecular Charge Transfer
INS	Structure Solution Instruction
LLT	Lower Limiting Threshold
LT	The Limiting Threshold
LUMO	Lowest Occupied Molecular Orbitals
NBO	Natural Bond Orbital
NLA	Nonlinear Absorption
NLO	Nonlinear Optical
NLR	Nonlinear Refraction
NPA	Natural Population Analysis
OL	Optical Limiting
ORTEP	Oak Ridge Thermal Ellipsoid Plot
RSA	Reverse Saturable Absorption
SHG	Second-Harmonic Generation
TD-DFT	Time-Dependent Density Functional Theory
THG	Third-Harmonic Generation
USM	Universiti Sains Malaysia
UV-VIS	Ultraviolet Visible
XRD	X-Ray Diffraction

LIST OF APPENDICES

SINTESIS, PENCIRIAN STRUKTUR DAN OPTIK

ANTRASENIL-KALKON BAHARU DENGAN JEJAMBAT

PENDERMA -π- PENERIMA UNTUK BAHAN OPTIK TIDAK LINEAR

ABSTRAK

Sebuah turutan terbitan antrasenil-kalkon baharu dengan sistem jambatan D−π−A telah berjaya disintesis menggunakan kaedah pemewapan Claisen-Schmidt, dan 10 hablur tunggal telah diperolehi. Struktur molekul terbitan antrasenil-kalkon ditentukan dan diperhalusi menggunakan kaedah pembelauan sinar-X (SCXRD) hablur tunggal. Sebatian tersebut dicirikan oleh padatan hablur, yang membentuk rangkaian molekul satu dimensi, dua dimensi atau tiga dimensi melalui interaksi antara molekul C—H···O, C—H···A, C—H··π, dan π···π. Semua sebatian menghasilkan jurang tenaga optik yang kecil dan jurang jalur tenaga HOMO-LUMO yang kecil, menjadikannya sangat polarisasi. Ikatan Orbit Semula Jadi (NBO) dan Analisis Populasi Semula Jadi (NPA) mendedahkan bahawa interaksi antara molekul intra- dan inter- mendorong pemindahan caj di antara molekul (ICT), dan menstabilkan semua sebatian untuk menghasilkan potensi optik taklinear (NLO) yang tinggi dengan interaksi penderma-penerima elektron yang lebih kuat, serta meningkat tenaga penstabilan. Kajian NLO menunjukkan penyahfokusan sendiri dan penyerapan tepu terbalik dalam semua sebatian dengan nilai $\chi^{(3)}$ (10^{-5} esu) yang lebih tinggi daripada penyelidikan terdahulu. Substituen pada molekul juga mempunyai kesan yang ketara ke atas aktiviti NLO peringkat ketiga mereka. Sebatian **2**, **3**, dan **10** dengan struktur molekul yang serupa, mengandungi atom bromin, menunjukkan nilai $\chi^{(3)}$ yang lebih tinggi daripada sebatian lain, menunjukkan peranan bromin dalam meningkatkan aktiviti NLO peringkat ketiga. Semua sebatian mempunyai potensi untuk aplikasi

penghad optik (OL) kerana lengkung ciri mereka menunjukkan keamatan cahaya berkurangan kepada sifar. Secara keseluruhan, bahan yang disintesis berpotensi untuk digunakan dalam pelbagai aplikasi seperti pengehad optik, penderiaan optik, pensuisan optik dan pemprosesan bahan.

SYNTHESIS, STRUCTURAL AND OPTICAL CHARACTERIZATION OF NOVEL DONOR-π-ACCEPTOR BRIDGED ANTHRACENYL-CHALCONES FOR NONLINEAR OPTICAL MATERIALS

ABSTRACT

A sequence of new anthracenyl-chalcone derivatives with a D−π−A bridge system has been successfully synthesized by using the Claisen-Schmidt condensation method and 10 single crystals have been successfully obtained. The molecular structure of the compounds was determined through single crystal X-ray diffraction (SCXRD) analysis. The compounds were characterized by their crystal packing, which formed one-dimensional, two-dimensional, or three-dimensional networks of molecules through intermolecular C—H···O, C—H···A, C—H··π, and π···π interactions. All compounds produced the small optical energy gap and the small HOMO)-LUMO energy band gap, making them highly polarizable. The study of Natural Bond Orbitals (NBO) and Natural Population Analysis (NPA) reveals that intra- and intermolecular interactions induce ICT and stabilize all compounds, resulting in high nonlinear optical (NLO) potential, with stronger electron donor-acceptor interactions increasing with stabilization energy. The NLO study showed self-defocusing and reverse saturable absorption in all compounds, with larger $\chi^{(3)}$ (10^{-5} esu) values than previous research. The substituents on a molecule also had a significant impact on their third-order NLO activity. Compounds **2**, **3**, and **10** with similar molecular structure, containing bromine atoms, showed higher $\chi^{(3)}$ values than other compounds, indicating bromine's role in enhancing third-order NLO activity. All compounds have potential for optical limiting applications, as their characteristic curve

shows light intensity decreases to zero. Overall, the synthesized materials have the potential to be used in various applications such as optical limiters, optical sensing, optical switching, and material processing.

CHAPTER 1

INTRODUCTION

1.1 Nonlinear Optical Materials

Nonlinear Optical (NLO) materials are a subject that is worth exploring for their fascinating properties. NLO studies light behavior in materials, focusing on polarization density response to the applied field, unlike linear optics which directly proportional to the applied field. The key characteristics and phenomena of NLO are nonlinear response (the polarization density of a material is not directly proportional to the applied electric field), high intensities laser, frequency conversion (nonlinear interactions can lead to the generation of new frequencies of light, such as second-harmonic generation, where a laser beam is converted to a beam with twice the frequency), phase conjugation (reversing the wavefront of a light beam, which can be used for image processing and optical communication), self-focusing (the focusing of a laser beam due to its own intensity, leading to higher intensities and potentially damaging effects), and optical solitons (stable pulses of light that can propagate without changing their shape or intensity). NLO were used in variety of applications such as laser technology, optical data storage, optical computing, and biomedical imaging. The most used properties for NLO studies are second-order NLO properties and third-order NLO properties (Naik et al. 2020). There has been a wide range of NLO materials that have been explored, like organic dyes, metal complexes of thiourea, gold nanoparticles, single crystals of organic molecules and more (Zainuri et al. 2018). For decades, NLO has been recognized as a potential topic with critical applications in the fields of optoelectronics (Singh et al. 2015) and photonics (Rajesh Kumar et al. 2012). Because of its application in optical data storage, optical processing, optical computing, sensor protection, optical switching, and other photonic

technologies, NLO has absolute significance in its area of research (Tejkiran et al. 2016). The modification of the nature of the incident light occurs when electromagnetic fields interact with matter, creating new field components with unique propagation characteristics. These NLO interactions have potential uses in optical systems and are significant from a technological standpoint.

Organic nonlinear materials have been researched for their NLO properties over semiconductor and inorganic materials for their large optical susceptibilities, high optical thresholds for laser power (Jayarama et al. 2013), low-energy transitions in the UV–vis region (Wang et al. 2013), ultrafast optical response times, easy to fabricate and synthetic adaptability in the creation of innovative materials (Vediyappan et al. 2021). The delocalization of electronic charge scattering that happens because of the intersection of orbitals in the π bond system of the basic organic NLO structure causes the high mobility of the electron density in the structure (Janarthanan et al. 2009). The improving asymmetric electronic scattering in either or both ground and excited states helps boost the optical nonlinearity by functionalizing both sides of the π bond system with suitable electron donor and acceptor groups. (Dhanaraj and Rajesh 2013).

In principle, susceptibility χ accounts for all optical material qualities and associated phenomena (absorption, refraction, reflection, scattering, and more). For materials, only the second-order NLO susceptibility, $\chi^{(2)}$ and third-order NLO susceptibility, $\chi^{(3)}$ were required for investigating the NLO characterization of organic materials (Nalwa 1991). $\chi^{(2)}$ created the second harmonic generation (SHG), while $\chi^{(3)}$ creating the third-harmonic generation (THG). SHG can occur in molecular assemblies that lack a symmetry centre (non-centrosymmetric) and must obey the crystal symmetry characteristics. However, there are no symmetry requirements for the occurrence of THG effects, which broadens the scope of $\chi^{(3)}$ investigations to

include a wide range of materials. Therefore, it is safe to use it $\chi^{(3)}$ to analyse the NLO properties of organic optical materials. (D.C Hanna 1981).

1.2 Anthracenyl-Chalcone Derivatives

Anthracene and its derivatives constitute a well-known class of materials with intriguing photophysical properties and have been extensively used in the creation of luminescent chemosensors and switches (Montalti et al., 2000). Anthracene is a type of polycyclic aromatic hydrocarbon that consists of three fused benzene rings sharing a common side. Polyaromatic hydrocarbons or π-conjugated materials are the major class of organic compounds because of their significant conductivity properties that have led to tremendous advancements in the field of organic electronics (Li et al. 2016).

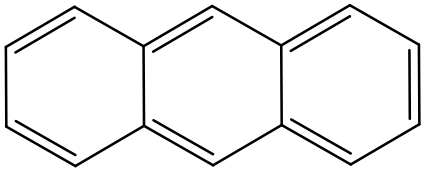

Figure 1.1 The molecular structure of anthracene (SNF Ab Rahman, 2023)

Most conjugated materials used in applications include light-emitting diodes (OLEDs) (Abhishek P. Kulkarni, 2004), field-effect transistors (OFETs) (Torrent and Rovira, 2008) and organic photovoltaic devices (OPVs), which are dependent on linear electron-rich fragments (Lin et al. 2017). Likewise, the optoelectronic features of π-conjugated systems have also been explored significantly because they open the door for low-cost, large-area, and flexible electronic devices (Wu et al. 2010). In recent decades, there has been significant ongoing research based on the new π-conjugated

systems, attributable to the constantly increasing number of applications in electronic devices as mentioned above.

Chalcone is α,β-unsaturated ketones, consisting of two aromatic rings (A and B) attached by α,β-unsaturated carbonyl system with a variety of substituents. In the chalcone molecule with a π-conjugated system, they deliver a large charge-transfer axis with suitable substituent groups on the terminal aromatic rings, which results in a strong intermolecular charge transfer (ICT) and may enhance the NLO properties (D'Silva et al. 2011).

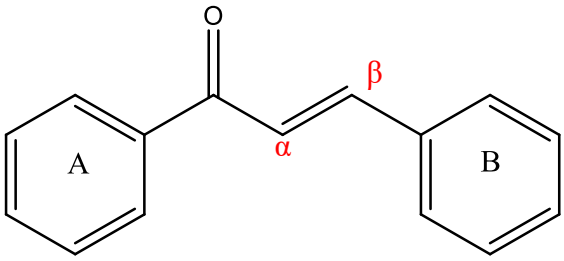

Figure 1.2 Basic structure of chalcone (SNF Ab Rahman, 2023)

Additionally, there is a lot of interest in π-conjugated molecular materials with fused rings in the developing field of organic electronics since their strong stability and good charge-carrier mobility may result in future optoelectronic applications (Wu, Liu, et al. 2010). Anthracenyl-chalcone molecules have a strong electron donor, a strong electron acceptor, and a highly polarizable π-conjugated bridge, which are the three conditions for significant nonlinear activity in an organic molecule (Sai Kiran et al. 2014). Anthracenyl-chalcones with a D–π–A bridge system are familiar organic NLO substances that have electron-donating and electron-accepting groups connected by a conjugated bridge that enables good interactions between the donor and acceptor moieties (Minato et al. 2017). Long-range charge transport occurs in the D-π-A bridge mechanism of π-delocalizing between anthracene and the acceptor, involving donor-

to-ligand and ligand-to-donor transfers. Furthermore, these electron donor groups and electron acceptor groups, contribute to the ICT between the two groups of opposite nature, which results in large optical nonlinearity. A novel system with high charge transfer is crucial as ICT between donor and acceptor will result in excellent optical properties (Ekbote et al. 2017). In such D-π-A molecules, ICT can be detected in even more distinctive optoelectronic properties (Bureš 2014).

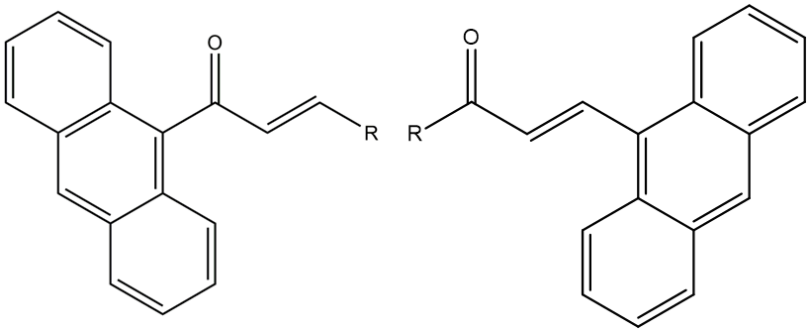

R: Different substituents of aldehyde/ketone.

Figure 1.3 Molecular structure of Anthracenyl-Chalcones (SNF Ab Rahman, 2023)

1.3 Synthesis of Anthracenyl-Chalcone Derivatives

Synthesis of anthracenyl-chalcone derivatives involves several methods, such as the Suzuki–Miyaura cross-coupling reaction (Tang et al. 2010), the carbonylative Sonogashira reaction (Wu, Neumann, et al. 2010), and the carbonylative Heck reactions (Schranck et al. 2012). For this research, the Claisen-Schmidt condensation reaction is used as this method are more environmentally sustainable option (green chemistry) (Winter et al. 2016), easy to prepare, produces a good yield of compounds, and can be conducted at room temperature (Jioui et al. 2016). This method also showed outstanding catalytic activity and recyclable catalysts (Jioui et al. 2016).

1.4 Problem Statement

Semiconductor and inorganic materials have been for more than a few decades on the market as NLO materials, yet they have flaws. Semiconductors like gallium arsenide are low in their NLO response time, even though they were the highest known as reduced dimensionality species (quantum wells or quantum wires) possess NLO effects (I.R.Whittall,1999). The difficulty in creating high-quality single crystals and putting them into electrical systems is one of the limitations of inorganic electro-optic devices (Raposo, 2016). Moreover, the cost of producing inorganic materials as single crystals is likewise high (Naik et al. 2020b).

The anthracenyl-chalcone derivatives of organic materials are explored as NLO materials to overcome the disadvantages of other materials. Anthracenyl-chalcone derivatives are in high demand among organic materials due to their fast response time, strong donor-acceptor intermolecular interaction, and a π-delocalized electron system that matches the requirements to facilitate optical nonlinearity (Mathew et al. 2022). It is also easy and low-cost to synthesis the organic materials and produce their single crystal.

1.5 Objectives

1. To synthesize and characterize anthracenyl-chalcone derivatives with D–π–A bridge system.
2. To investigate the NLO properties of the anthracenyl-chalcone derivatives.
3. To determine the structure-activity relationship between the NLO properties and the crystal structure.

CHAPTER 2

LITERATURE REVIEW

2.1 Single crystal X-Ray Structure of Chalcone Derivatives

The molecular structure of chalcones can be present in various forms involving *cis*, *trans*, *s-cis*, and *s-trans* configurations (Figure 2.1). In chalcones, the hydrogen atoms of the double C_α=C_β bond are present in the *cis* or *trans* configuration, while in the C=O bond, the hydrogen atoms are present in the *s-cis* or *s-trans* configuration for the vinylenic double bond due to free rotation of the single bond between C-carbonylic and C_α (Evranos Aksöz & Ertan, 2011). *S-cis* confirmation is the most stable conformer and appears to be completely planar. Meanwhile, the *trans*-(*s-cis*)-chalcone is the most stable among the experimentally known isomers of chalcone (Evranos Aksöz & Ertan, 2011).

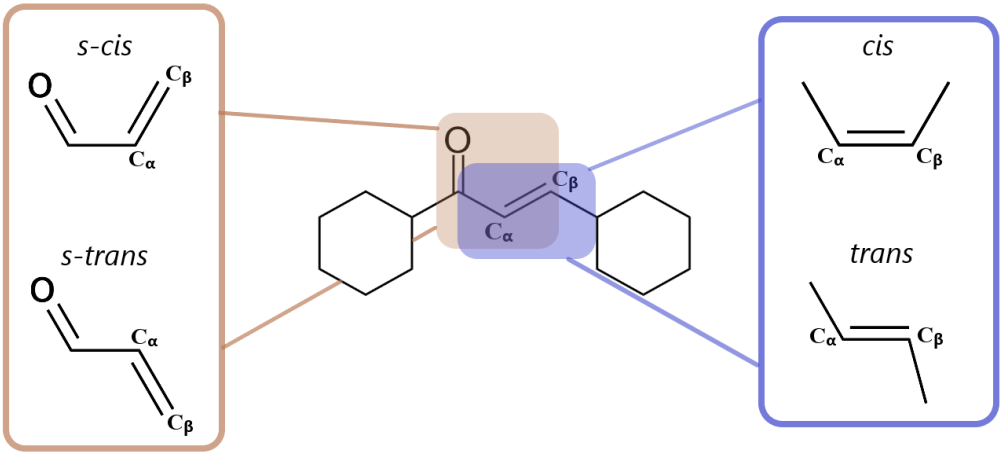

Figure 2.1 Configuration type in chalcone (SNF Ab Rahman, 2023).

The different types of single crystals with the *cis* (Figure 2.2a) and *trans* (Figure 2.2b) isomers of the chalcone derivatives named 1-(5-bromothiophen-2-yl)-3-(10-chloroanthracen-9-yl) prop-2-en-1-one have been reported by (Naresh et al., 2021).

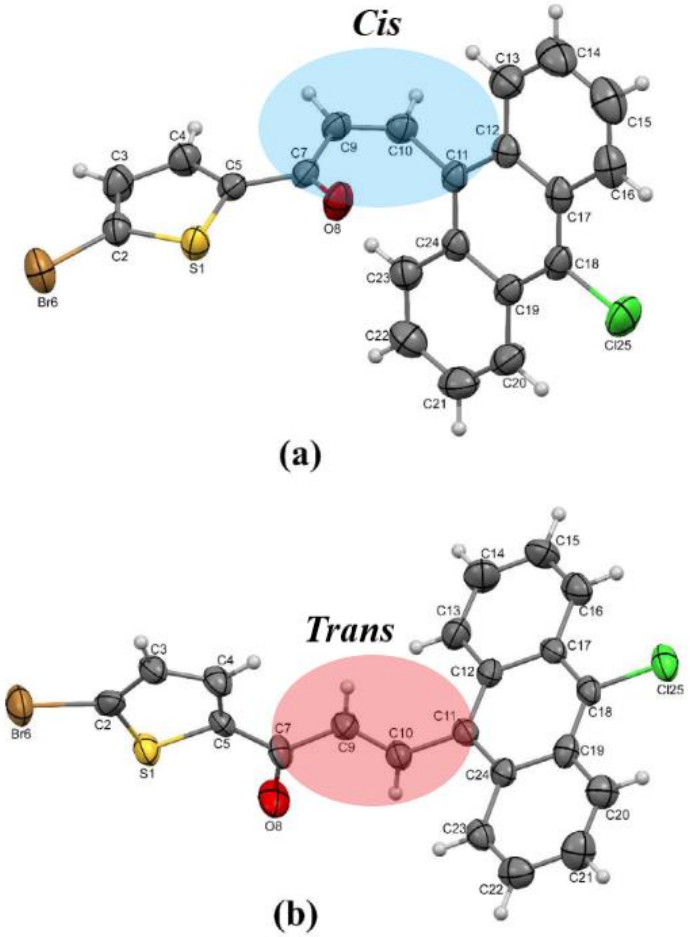

Figure 2.2 Molecular structure of (a) *cis* and (b) *trans* isomers of 1-(5-bromothiophen-2-yl)-3-(10-chloroanthracen-9-yl) prop-2-en-1-one (3) (Naresh et al., 2021).

Besides, the molecule named (*E*)-1-(Benzo[d][1,3]dioxol-5-yl)-3-([2,2′-bi-thio-phen]-5-yl)prop-2-en-1-one has shown an *s-cis* configuration within the enone moiety and a large planar structure at the molecule, as mentioned in Anizaim et al., 2019 (Figure 2.3).

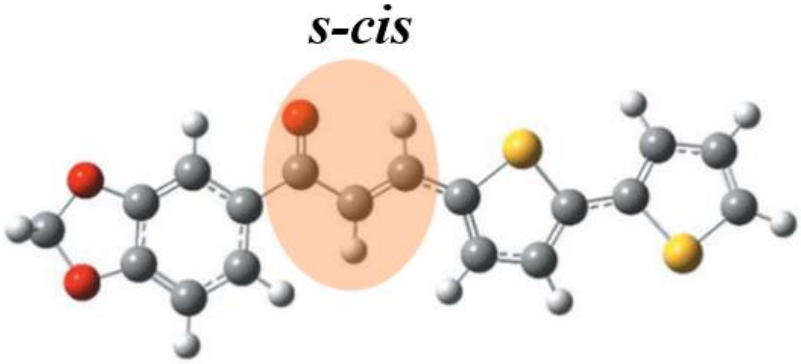

Figure 2.3 Molecular structure of (*E*)-1-(Benzo[d][1,3]dioxol-5-yl)-3-([2,2′-bi-thio-phen]-5-yl)prop-2-en-1-one with *S-cis* configuration (Anizaim et al., 2019).

Furthermore, Zainuri et al., 2018 outline two compounds with *s-trans* conformation: (*E*)-1-(anthracen-9-yl)-3-(2,4-dichlorophenyl)prop-2-en-1-one and (*E*)-1-(anhracen-9-yl)-3(2,6-dichlorophenyl)prop-2-en-1-on (Figure 2.4). Both compounds show a highly twisted planar structure at the enone bridge due to the bulkiness of the anthracene ring.

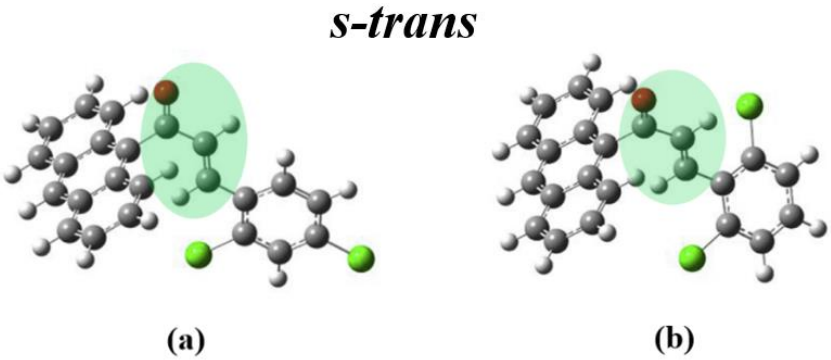

Figure 2.4 Molecular structure of (a) (*E*)-1-(anthracen-9-yl)-3-(2,4-dichlorophenyl)prop-2-en-1-one and (b) (*E*)-1-(anhracen-9-yl)-3(2,6-dichlorophenyl)prop-2-en-1-on with *s-trans* conformation (Zainuri et al., 2018).

2.2 Crystal Packing of Chalcone Derivatives

Analyzing the crystal packing and molecular structure of chalcones provides a deeper understanding of intermolecular charge transfer (ICT) and how it affects NLO. Based on a study by Alsaee et al., 2022 crystal packing of C─H···O, C─H···Br, and parallel π···π weak interaction were found in 1-(4′-bromo-[1,1′-biphenyl]-4-yl)ethan-1-on (Figure 2.5). The hydrogen bonds of C─H···O, C─H···Br, and parallel π···π stacking within the crystal packing allow the molecules to interact in a head-tail manner, which allows for efficient charge transfer within the crystal, with a face-face arrangement. C─H···O interaction also has the strongest interaction between the molecules, which helps increase the ICT of the compounds.

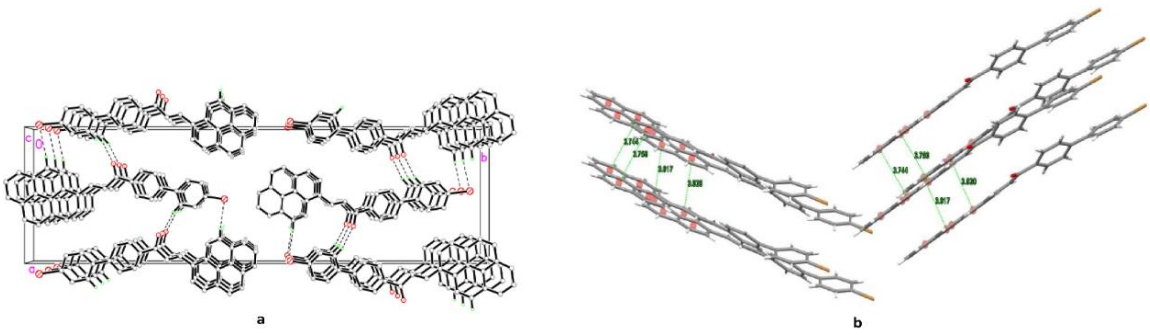

Figure 2.5 Crystal packing of 1-(4′-bromo-[1,1′-biphenyl]-4-yl)ethan-1-on with (a) C─H···O, C─H···Br interactions in a chain pattern along the b-axis and (b) π ···π interactions in a face-to-face stacking pattern (Alsaee et al., 2022).

The crystal packing of (*E*)-1-(anthracen-9-yl)-3-(2,4-dichlorophenyl)prop-2-en-1-one was connected by C─H···O (Figure 2.6a) meanwhile, (*E*)-1-(anthracen-9-yl)-3(2,6-dichlorophenyl)prop-2-en-1-one was connected C─H···π interactions (Figure 2.6b) (Zainuri et al., 2018). As mentioned in the paper, due to the side-by-side packing of crystals in (*E*)-1-(anthracen-9-yl)-3-(2,4-dichlorophenyl)prop-2-en-1-one was

exhibiting a higher nonlinear refractive index than (*E*)-1-(anthracen-9-yl)-3(2,6-dichlorophenyl)prop-2-en-1-one.

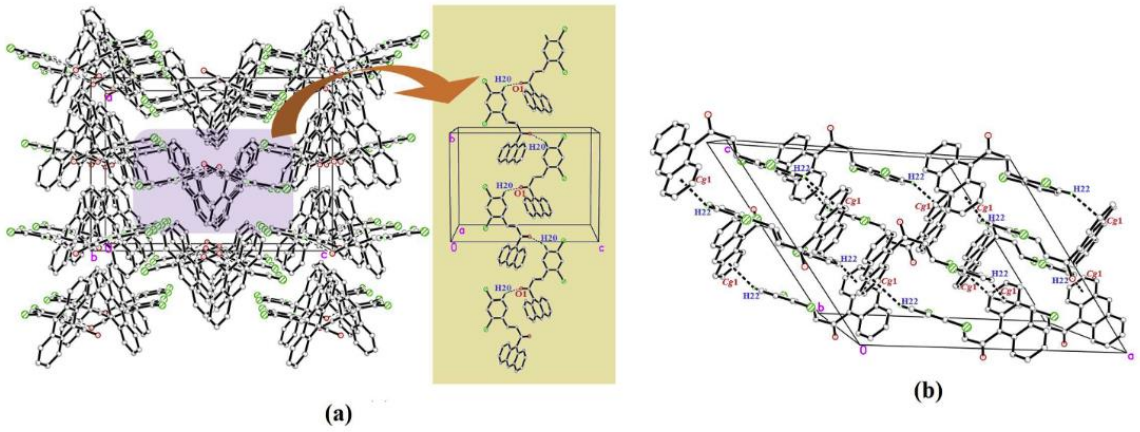

Figure 2.6 Crystal packing of compound (a) (*E*)-1-(anthracen-9-yl)-3-(2,4-dichlorophenyl)prop-2-en-1-one with C─H···O and (b) (*E*)-1-(anthracen-9-yl)-3(2,6-dichlorophenyl)prop-2-en-1-one with C─H···π interactions (Zainuri et al., 2018).

Furthermore, crystal packing with the presence of strong electron donating groups and a supramolecular layer with intermolecular N─H···O and C─H···O hydrogen bonds in the crystal packing increases the NLO properties (Figure 2.7) (Ekbote et al., 2017).

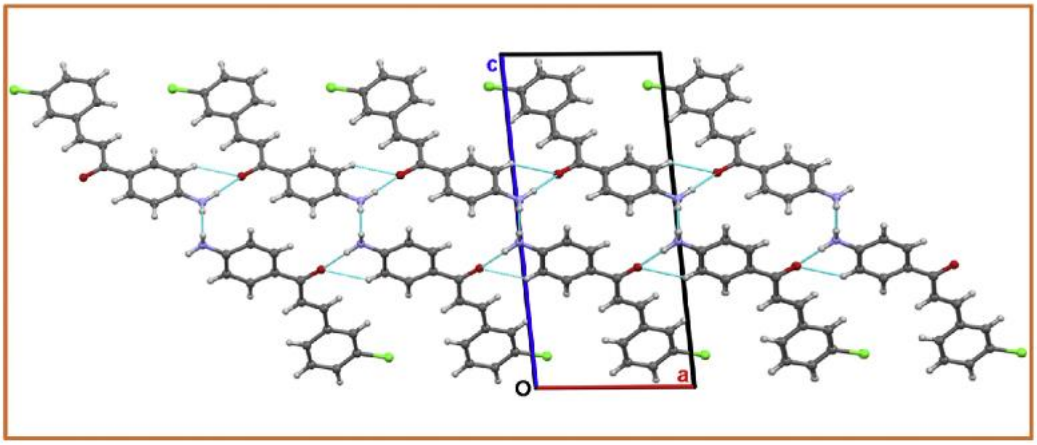

Figure 2.7 Crystal packing of (*E*)-1-(4-aminophenyl)-3-(3-chlorophenyl) prop-2-en-1-one with N─H···O and C─H···O hydrogen bonds along the b-axis (Ekbote et al., 2017).

Moreover, Chidan Kumar et al., 2017 reported that the crystal structure in which the molecules were connected by an intermolecular C–H···O hydrogen bond in an inversion dimers pattern may be the reason for the high values of NLO parameters (Figure 2.8).

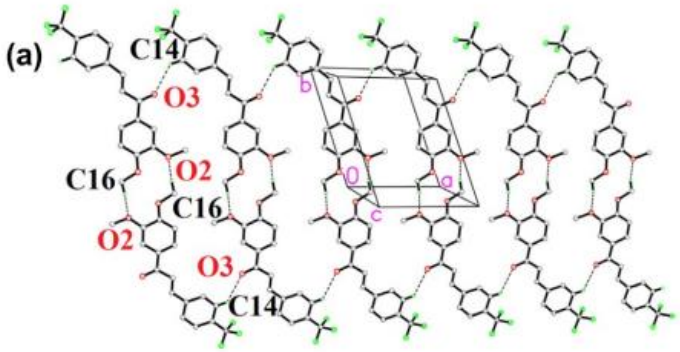

Figure 2.8 Crystal packing of (*E*)-1-(3,4-dimethoxyphenyl)-3-(4-(trifluoromethyl)phenyl) prop-2-en-1-one with C16–H16A···O2 and C16–H16A···O2 hydrogen bond inversion dimer (Chidan Kumar et al., 2017).

2.3 UV-Visible Spectroscopic Studies of Chalcone Derivatives

A UV-visible spectrophotometer measures the absorbance or transmittance of light passing through a medium (Rocha et al., 2018). Most organic molecules and functional groups are transparent in the UV-visible parts of the electromagnetic spectrum, which are the areas where wavelengths vary from 190nm to 800nm (Pavia et al., 2000). Table 2.1 shows the maximum absorption and the energy band gap of anthracenyl chalcones from earlier research.

Table 2.1 The λ_{max} (in nm) and energy band gap (in eV) of anthracenyl chalcones from earlier research.

Literature	Maximum absorption, λ_{max} (nm)	Energy gap (eV)
(Zainuri et al., 2018)	386, 387	3.03
(Patil et al., 2020)	379	3.9
(Lee et al., 2021)	388, 387	2.97, 2.76
(Mathew et al., 2022)	369, 375, 348, 356	3.17, 3.16, 3.17, 3.17

Zainuri et al., 2018 reported absorption wavelengths at 386 and 387 nm and an energy gap of 3.03 eV. The crystal displays strong absorption in the UV region due to the absorption bands associated with the aromatic ring and the presence of C=O groups (n-π* and π-π* transitions). Also, it found that substitution position at the *o*, *p* (I) and *o*, *o* (II) of electron-withdrawing chloro groups affects maximum absorption values. Meanwhile, Patil et al., 2020 reported the derivation of three diverse types of chalcones, including anthracenyl chalcone. The maximum absorption wavelength of anthracenyl chalcone was 379 nm with a 3.9 eV energy gap. A Tauc's plot was used to determine each chalcone's energy band gap (Figure 2.9).

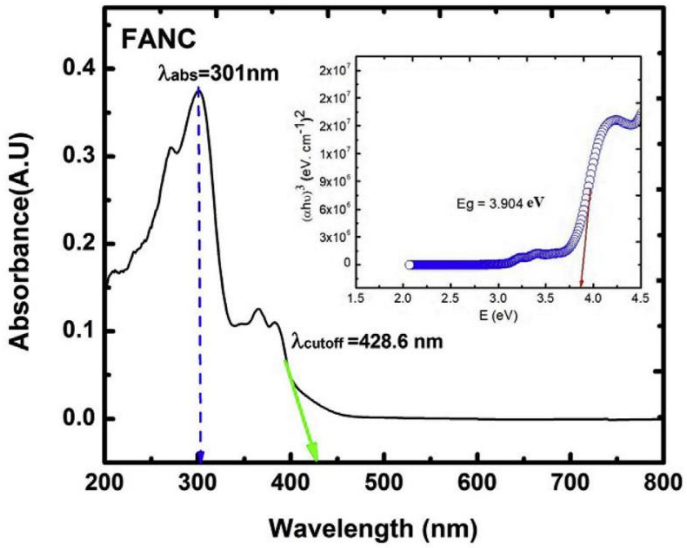

Figure 2.9 UV-visible absorption spectra of anthracenyl chalcone (FANC) with the inset of Tauc's plot (Patil et al., 2020).

Lee et al., 2021 reported 388 nm and 387nm as the maximum absorption wavelengths and energy gaps at 2.97 and 2.76 eV. Because the benzene ring in the anthracenyl chalcone is π-conjugation, its existence of benzene ring would somehow lengthen the length of π conjugate planar geometry and reduce the energy of the system by improving the capacity of carbazole units to remove electrons. Moreover, (Mathew et al., 2022b) reported different types of solvents for UV-vis absorption analysis. Analysis showed the absorption bands and energy gaps for CCl4 (369 nm, 3.17 eV), toluene (375 nm, 3.16 eV), acetone (348 nm, 3.17 eV), and DMSO (356 nm, 3.17 eV) solvents. The maximum absorption wavelength is assigned π - π∗ transitions, which are attached to the C=O group and aromatic ring excitation.

Additionally, Filpponen et al., 2011 reported the UV light absorption spectra of CNCs, anthracene, and CNC-Anthracene have revealed that the UV light absorption spectra of modified CNCs have the same absorption wavelength as those of the control anthracene (typical at 392 nm, 372 nm, 355 nm, and 338 nm), whereas there is no UV absorption in the unmodified CNCs (Figure 2.10).

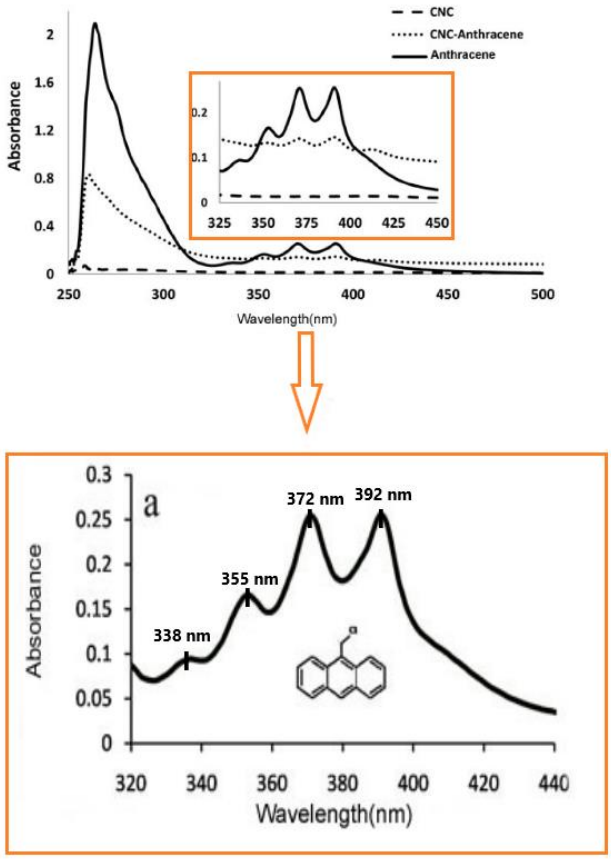

Figure 2.10 UV light absorption spectra of anthracene (solid line, orange box), CNC-Anthracene (dotted line) and CNCs (dashed line) (Filpponen et al., 2011).

2.4 Density Functional Theory (DFT) Studies of Chalcone Derivatives

2.4.1 Highest Occupied Molecular Orbitals (HOMO)-Lowest Occupied Molecular Orbitals (LUMO) energy band gap

HOMO-LUMO energy gaps determine chemical reactivity and explain the actual charge transfer interactions within molecules. The process of electronic absorption happens when the HOMO and LUMO electrons are excited by one electron. Electron donors are represented by HOMO, while electron acceptors represent LUMO (Mathew et al., 2019).

Based on Table 2.2, the previous studies show values for the HOMO-LUMO energy gap. All research reported a small HOMO-LUMO energy gap, which is good for NLO properties. Previous studies have shown that molecules with a smaller HOMO-LUMO energy gap, strong chemical reactivity, soft molecules, and polarizable properties but weak kinetic stability exhibit large ICTs and increased NLO activities (Zainuri et al., 2022, Mathew et al., 2019, Maidur et al., 2018, Lee et al., 2021).

Table 2.2 HOMO-LUMO energy gap values from the previous study.

Previous Research	**HOMO-LUMO Energy Gap (eV)**
Zainuri et al., 2022	2.48 – 2.97
Mathew et al., 2022	3.03
Lee et al., 2021	2.74 – 2.98
Mathew et al., 2019	3.16 – 3.17
Maidur et al., 2018	3.06 – 3.10

According to Mathew et al., 2019 analysis of two anthracenes containing the substituent units methoxy-phenyl and ethoxy-phenyl, the HOMO is located in the anthracene group, and the LUMO is in the methoxy-substituted benzene ring and the keto-ethylene group (Figure 2.11). These compounds also have low kinetic stability, high chemical potential, outstanding chemical strength, and a softness parameter that contributes to a high ICT, and increased NLO activity. Mathew et al., 2022 also stated that anthracene chalcone with a biphenyl substituent was a soft molecule, with strong chemical reactivity but weak kinetic stability.

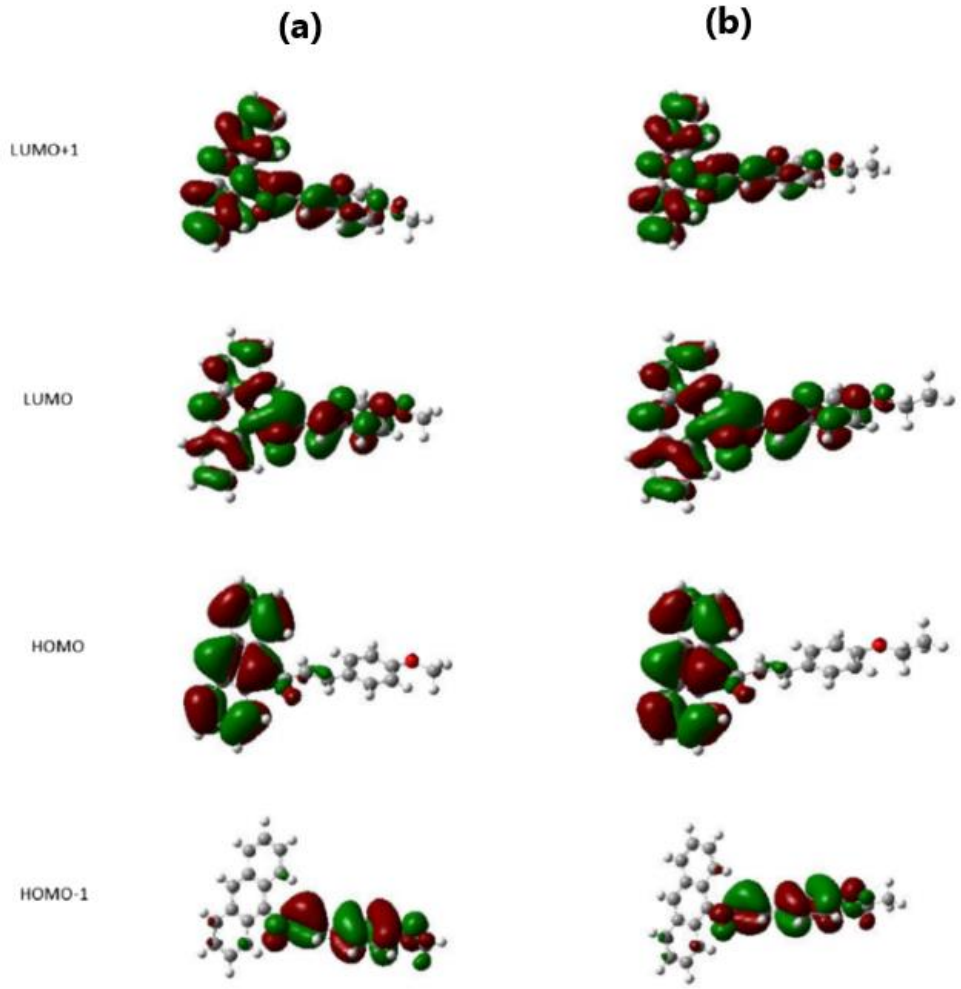

Figure 2.11 The Frontier Molecular orbitals of two anthracene containing the substituent units (a) methoxy-phenyl and (b) ethoxy-phenyl (Mathew et al., 2019).

Additionally, Zainuri et al., 2022 reported that one of the three heterocyclic anthracene chalcones displays higher softness with a lower energy gap than the other compounds. This makes it the most reactive and most polarizable relative to other compounds. As stated by Maidur et al., 2018, the HOMO is located in the anthracene group, the LUMO is located on the halogenated (Br & Cl) substituted benzene ring, and the carbonyl group and the small energy gap suggest the molecules are soft.

2.4.2 Natural Bond Orbital (NBO)

NBO study is one of the most important indicators because it enables the investigation of the electronic distribution within a given molecule. This study enables the exploration the intra- and intermolecular interactions between the electron donors and acceptors of that molecule (Lee et al., 2021). The NBO analysis examines interactions between occupied (donor) Lewis-type NBOs and unoccupied (acceptor) non-Lewis NBOs, with lone pairs and two-center bonds representing the chemical bonding for a single Lewis structure (Glendening et al., 2013). The Non-Lewis set consists of unoccupied valence nonbonding (LP*), extra-valence-shell Rydberg (RY*) orbitals, and the valence antibonding (BD*) (Glendening et al., 2013). The NBO 3.0 program, created by Weihnold and colleagues, was used to conduct NBO analysis (Carpenter & Weinhold, 1988). Intramolecular interactions that happen between donors and acceptors will stabilize the whole molecule, improving its NLO activity (Mathew et al., 2022b).

As reported by Aditya Prasad et al., 2015, the orbital overlap of the π(C─C) and π^*(C─C) bond orbitals provide insight into the intramolecular hyper-conjugative interactions, which stabilize the (1E,4E)-1,5-di-p-tolylpenta-1,4-dien-3-one (DTDO) (Figure 2.12) through an intramolecular charge transfer. Furthermore, the electron density of DTDO (1.99 e) shows strong delocalization from donor σ(O1–C2) to acceptor σ*(C2–C3) due to the strong intramolecular hyper-conjugative interactions of π-electrons. This high electron density could be the reason for the high electronegativity environment. The oxygen lone pair O1 has the greater interaction energy contribution in their π* to π antibonding orbitals.

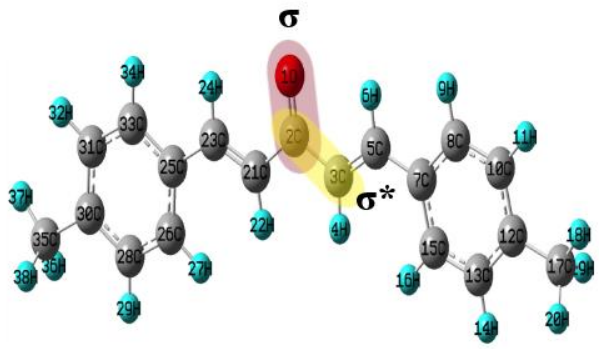

Figure 2.12 Optimized geometry (1*E*,4*E*)-1,5-di-p-tolylpenta-1,4-dien-3-one (DTDO) (Aditya Prasad et al., 2015)

2.4.3 Natural Population Analysis (NPA)

NPA is the mathematical technique for dividing up and distributing electron density that offers better electron distribution and numerical stability (Reed et al., 1988). It is an alternative to conventional Mulliken population analysis and provides better numerical stability and electron distribution in compounds of high ionic character, such as metal atoms (Reed et al., 1985).

Based on previous studies on NPA by Mathew et al., 2022, all carbon atoms have negative values except for C1, and all hydrogen atoms have a positive charge. The positive charge carbon atom, C1 connected to the O4 atom (Figure 2.13) indicates the protonation spot. Since the donor and acceptor groups have different atomic charges, a charge transfer mechanism occurs within the molecule, hence the analysed chalcone exhibits a nonlinear optical response.

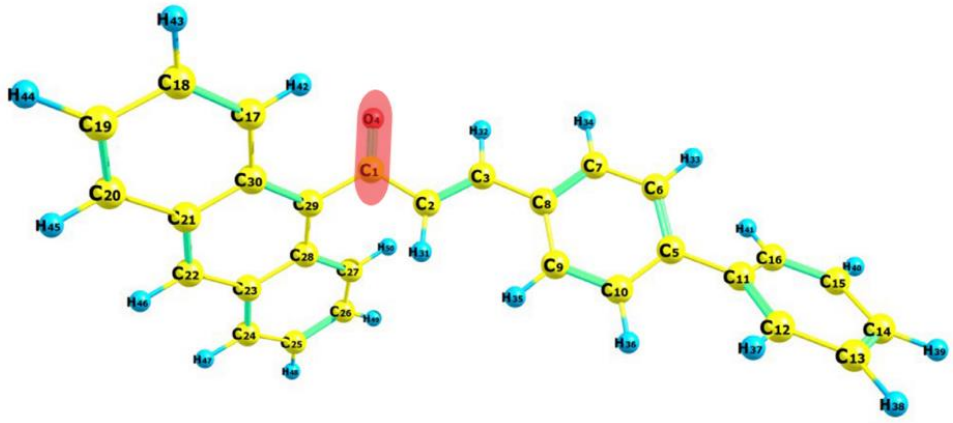

Figure 2.13 Optimized geometry of (2*E*)-1-(Anthracen-9-yl)-3-(biphenyl-4-yl)prop-2-en-1-one (Mathew et al., 2022).

In Mathew et al., 2019 studies indicate that positive carbon atom bonded with the oxygen atom, O4 and O11 indicates protonation location. Both molecules undergo charge transfer because of the atomic charge distribution of donor and acceptor groups. As a result, an NLO response is generated.

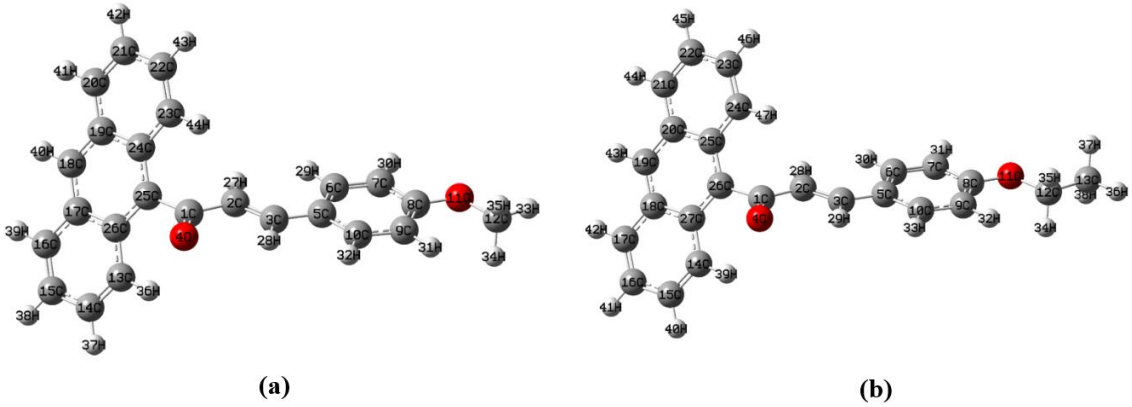

(a) **(b)**

Figure 2.14 Optimized geometry of (a) (2*E*)-1-(Anthracen-9-yl)-3-(4-methoxyphenyl) prop-2-en-1-one and (b) (2*E*)-1-(Anthracen-9-yl)-3-(4-ethoxyphenyl)prop-2-en-1-one (Mathew et al., 2019).

2.5 Nonlinear Optical (NLO) Studies of Chalcone Derivatives

The z-scan method is used to investigate third-order NLO properties due to its simplicity and sensitivity (Arshad et al., 2017). This method has the benefit of immediately indicating the type and sign of the optical nonlinearity. It can identify the sign and magnitude of the nonlinear refractive index (n_2) and nonlinear absorption coefficient (β) simultaneously. (Maidur et al., 2018 ,Naik et al., 2020). In the meantime, optical liming refers to the reduction in transmission of organic materials as incident light increases (Alsaee et al., 2023). Optical limiting materials, such as RSA (reverse saturable absorption) and NLR (nonlinear refraction), are important for defocusing and self-focusing due to their technological importance (Wong et al., 2022). Table 2.3 listed the NLO analysis from the previous studies.

Table 2.3 NLO analysis from the previous studies.

Literature	$\boldsymbol{\beta}$ **(cm/W)**	$\boldsymbol{n_2}$ **(cm^2/W)**	$\boldsymbol{Re\ x^{(3)}}$ **(esu)**	$\boldsymbol{Im\ x^{(3)}}$ **(esu)**	$\boldsymbol{x^{(3)}}$ **(esu)**	**OL (W/cm^2)**
(Wong et al., 2022) (I) 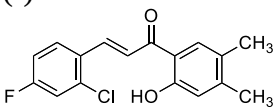 (II) 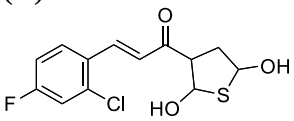 (III) 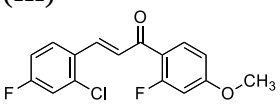	1.72, 1.90, 2.45 $\times 10^{-5}$	2.50, -0.14, -1.14 $\times 10^{-9}$	13.00, 0.74, 5.95 $\times 10^{-8}$	0.38, 0.42, 0.54 $\times 10^{-8}$	13.00, 0.85, 5.97 $\times 10^{-8}$	2.37, 2.37, 2.37 $\times 10^{4}$
(Zainuri et al., 2023) (NP1) 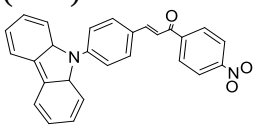 (NP2)	1.50, 1.88 $\times 10^{-5}$	-3.80, -4.08 $\times 10^{-10}$	3.26, 3.50 $\times 10^{-9}$	2.05, 2.57 $\times 10^{-6}$	2.05, 2.57 $\times 10^{-6}$	235, 168 $\times 10^{-3}$

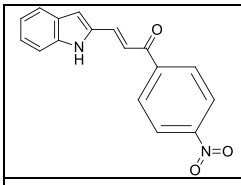						
(Alsaee et al., 2023) 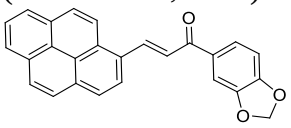 Solvent: Toluene, DCM, Acetone, DMSO	1.15, 10.00, 0.91, 1.79 $\times 10^{-4}$	-1.96, -0.013, -1.35, -1.84 $\times 10^{-7}$	-2.23, -1.58, -1.87, -2.14 $\times 10^{-8}$	-1.47, -1.26, -1.043, -2.45 $\times 10^{-6}$	1.48, 1.26, 1.052, 2.45 $\times 10^{-6}$	1376, 1360, 1335, 1398 $\times 10^{-3}$
(Mathew et al., 2022b) 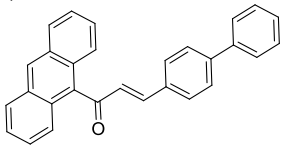 Solvent: DMSO, Acetone, Toluene, CCl_4	5.35, 15.77, 3.25, 2.35 $\times 10^{-12}$	15.03, 9.35, 2.92, 2.77 $\times 10^{-19}$	9.23, 6.06, 1.24, 1.11 $\times 10^{-13}$	1.39, 4.32, 0.58, 0.40 $\times 10^{-13}$	9.33, 7.44, 1.37, 1.18 $\times 10^{-13}$	9.93, 5.79, 11.72, 15.07

Based on Wong et al., 2022, Compound III shows higher NLA (nonlinear absorption) behaviour compared to compounds I and II. The values for compounds I, II and III are 33.48×10^{-8}, 1.97×10^{-8} and 15.33×10^{-8} esu, respectively. It was determined that compound I has a higher electron-donating capacity in contrast to normal chalcone, resulting in a generous ICT in D–π –A–π –A configuration. This paper also predicted that the chloro group in compound II would be weaker compared to another halogen group. The continuous wave (CW) regime shows negative nonlinearities for all chalcone derivatives. In contrast to the other chalcones, compound III exhibits the largest NLA response and is better at optical limiting.

From Zainuri et al., 2023 , (E)-3-(1H-indol-2-yl)-1-(4-nitrophenyl)prop-2-en-1-one (NP2) with the fused ring attached has higher $\chi^{(3)}$ value of compared to (E)-3-[4-(9,9a-dihydro-8aHcarbazol-9-yl)phenyl]-1-(4-nitrophenyl)prop-2-en-1-one (NP1). The studies also conclude that a donor part containing electron-withdrawing groups enhances optoelectronic properties. Based on the optical limiting analysis described in

the article, NP2 has a lower threshold and higher β values than NP1. The lower optical limiting threshold and higher β values explain that NP2 has faster-limiting behaviour with large optical nonlinearity.

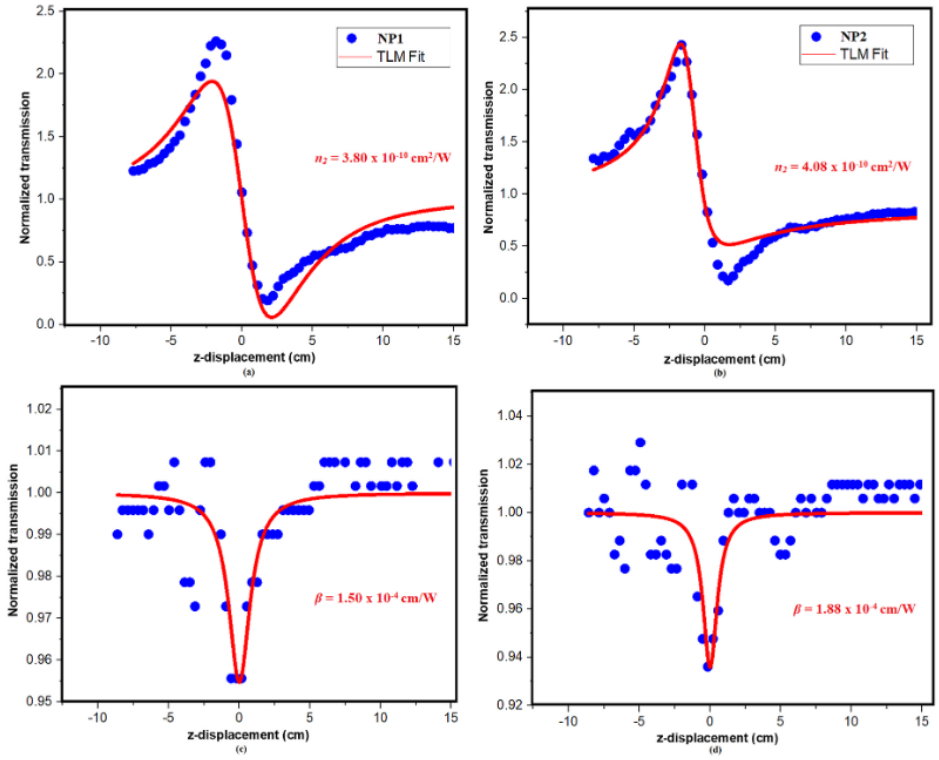

Figure 2.15 Closed Aperture and Open Aperture of NP1 (a, c) and NP2 (b,d) (Zainuri et al., 2023).

Alsaee et al., 2023 studied the NLO value effect in different types of solvents (toluene, DCM, acetone, and DMSO). There are increases in solvent polarity in the order of DCM, acetone, and DMSO excluding toluene solvent. Probably this is due to the strong delocalized π-electrons, π-π interactions between electrons, and H-bonds in pyrene-based chalcones. Acetone solvent produces the lowest optical limiting value, while DMSO solvent produces the highest (1398 W/cm^2) optical limiting value (Figure 2.16). DMSO is therefore highly polarized and better for NLO analysis.

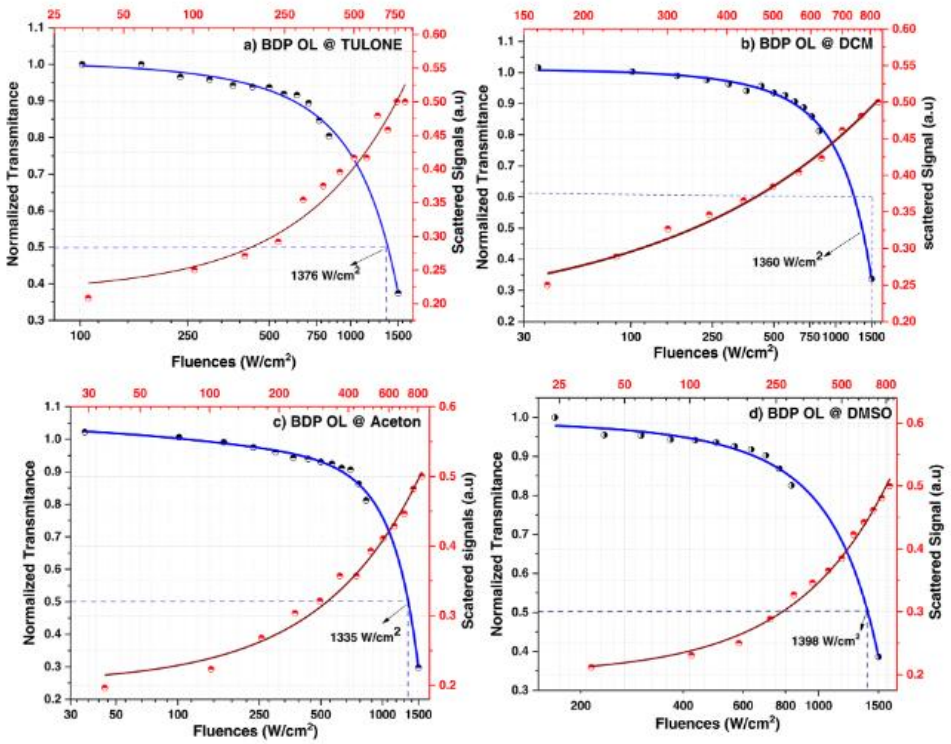

Figure 2.16 Optical limiting curves of (*E*)-1-(benzo[d][1,3]dioxol-5-yl0-3-(pyren-1-yl)prop-2-en-1-one in a) Toluene, b) Dichloromethane (DCM), c) Acetone and d) Dimethyl sulfoxide (DMSO) solvent (Alsaee et al., 2023).

Mathew et al., 2022 reported NLO analysis on (2*E*)-1-(Anthracen-9-yl)-3-(biphenyl-4-yl)prop-2-en-1-one [biphenyl-ANC] in DSMO, acetone, toluene, and CCl_4 solvents. DSMO have the highest value of $\chi^{(3)}$(9.33×10^{-13} esu) compared to other solvents. The investigated chalcone derivative has a higher third-order susceptibility $\chi^{(3)}$ than dibenzylideneacetone and its derivatives by one order. Biphenyl-ANC chalcone's third-order NLO characteristics were equivalent to those of previously known chalcones based on anthracene. Biphenyl-ANC exhibits strong optical limiting behaviour, with the nonlinear absorption coefficient dependent on the solvent used. This is similar to that of the reported anthracenyl chalcone derivative.